Turbulent flow at 190 m height above London during 2006–2008: a climatology and the applicability of similarity theory

C. R. Wood*[1], A. Lacser[1,2], J. F. Barlow[1], A. Padhra[1], S. E. Belcher[1], E. Nemitz[3], C. Helfter[3], D. Famulari[3], C. S. B. Grimmond[4]

[1] Department of Meteorology, University of Reading, Reading, RG6 6BB, UK

[2] Permanent affiliation; Israel Institute for Biological Research. Ness-Ziona, Israel

[3] Centre for Ecology and Hydrology (CEH) Edinburgh, Bush Estate, Penicuik, EH26 0QB, UK

[4] King's College London, The Strand, London, WC2R 2LS, UK

* Corresponding author: Curtis R. Wood, c.r.wood@reading.ac.uk, +44 118 378 6721

Abstract   Flow and turbulence above urban terrain is more complex than above rural terrain, due to the different momentum and heat transfer characteristics that are affected by the presence of buildings (e.g. pressure variations around buildings). The applicability of similarity theory (as developed over rural terrain) is tested using observations of flow from a sonic anemometer located at 190.3 m height in London, U.K. using about 6500 hours of data.

Turbulence statistics—dimensionless wind speed and temperature, standard deviations and correlation coefficients for momentum and heat transfer—were analysed in three ways. First, turbulence statistics were plotted as a function only of a local stability parameter z/Λ (where Λ is the local Obukhov length and z is the height above ground); the σ_i/u_* values ($i=u,v,w$) for neutral conditions are 2.3, 1.85 and 1.35 respectively, similar to canonical values. Second, analysis of urban mixed-layer formulations during daytime convective conditions over London was undertaken, showing that atmospheric turbulence at high altitude over large urban cities might not behave dissimilarly from that over rural terrain. Third, correlation coefficients for heat and momentum were analyzed with respect to local stability.

The results give confidence in using the framework of local similarity for turbulence measured over London, and perhaps other cities. However, the following caveats for our data are worth noting: (i) the terrain is reasonably flat, (ii) building heights vary little over a large area, and (iii) the sensor height is above the mean roughness sublayer depth.

Keywords   Mixed-layer · Similarity theory · Urban boundary layer · Urban meteorology · Urban turbulence

1 Introduction

The effort to study urban micrometeorology has been increasing in recent years, since it is essential to understand flow and turbulence characteristics in urban areas in order to provide better predictions for thermal comfort and human exposure to hazardous materials. To understand and model the flow and dispersion in such environments—and its coupling to both the roughness elements and to the outer flow—the following work tests the validity of similarity relationships based on local Monin-Obukhov theory (e.g. Roth 2000; Al-Jiboori et al. 2002), which is often assumed to hold despite the inhomogeneity of urban surfaces.

Monin-Obukhov similarity theory is a powerful tool to predict turbulence statistics in the horizontally-uniform surface layer. Numerical models, from local and mesoscale to global models, use the Monin-Obukhov formulations to relate surface fluxes of momentum, heat and water vapour to meteorological variables. There is still some uncertainty of the applicability of this theory in urban areas where there is greater inhomogeneity in surface roughness and thermal features (both in terms of spatially-inhomogeneous sensible heat flux and anthropogenic heat production). To enable comparisons of turbulence statistics from observations at different locations, appropriate scaling is necessary. Monin-Obukhov formulations can be extended to local similarity by using the local velocity scale (u_*), local temperature scale (T_*) and the local Obukhov length (Λ), so that similarity is defined for a specific height rather than the entire inertial sublayer.

Following measurements taken over Beijing at 47–280 m (Al-Jiboori et al. 2002), dimensionless quantities such as velocity and temperature standard deviations were represented as a function only of a local stability parameter $\zeta = z'/\Lambda$ ($z' = z - z_d$, z is the height above ground and z_d is the zero-plane displacement (22 m in that case)). Quan and Hu (2009), analyzing more recent data from the same tower, argued that the relationships between fluxes and variances provide more detail about the dynamic and thermal effects on urban flow and this approach might be a better way to characterize turbulence in the urban boundary layer than using Monin-Obukhov similarity theory.

Some recent relationships between normalized wind and temperature standard deviations and ζ based on urban measurements are relevant; in particular, measurements at 47 m in Quan and Hu (2009) and a review for unstable conditions ($0.05 < -\zeta < 6.2$) for measurements about 2.5 times the building height in Roth (2000). These urban relationships are given in Table 1 with studies from simpler terrain, where u_* is the local friction velocity, the temperature scale is $T_* = -(\overline{w'T'})_0 / u_*$, $i = u, v, w$ (velocity components of streamline, spanwise and vertical flow) and $(\overline{w'T'})_0$ is the mean

surface kinematic heat flux (w' and T' are fluctuations about the means). The overbar is a time mean, and the subscript zero represents a surface value.

Analysis of data taken during neutral conditions in Oklahoma City (Chang et al. 2009) showed that σ_i / u_* decreased with height (Table 2), while analysis of data from the same tower (Lundquist et al. 2004) showed larger values compared with other cities surveyed by Roth (2000). They argued that this might have been because the tower was located 500 m downstream of the tallest buildings in Oklahoma City (of height 100 m) and the enhanced turbulent kinetic energy (and increase in u_*) was primarily experienced by the flow moving through the city centre and not by the flow downstream in the vicinity of the tower. Hanna and Zhou (2007) analyzed sonic anemometer observations at street level and at rooftops from the March 2005 Madison Square Garden (MSG05) and August 2005 in Midtown Manhattan (MID05) urban dispersion field campaigns. They found that, for daytime conditions and for either surface or rooftop anemometers, most of the dimensionless turbulence averages are very similar (within about 20%) for MSG05 and MID05. It seems that the dimensionless turbulence averages are similar (Table 2) although taken at different sites, implying consistency from one urban area to another, and suggesting that similarity relationships are valid.

Further away from the urban surface, mixed-layer scaling—and the influence of the boundary-layer depth—is expected to be more important in the scaling of turbulence data. For convective conditions, Clarke et al. (1982) suggested using the peak wavelength in the spectra of u and v as a proxy for the mixed-layer depth (z_i) and proposed the relationship $\sigma_u = C_u (u_*^3 \lambda_{\max} /(\kappa z) + w_*^3)^{1/3}$, where w_* is the convective velocity scale (defined later), $\lambda_{\max}$ is the wavelength of the spectral energy peak (see later) and κ is the von Kármán constant (0.41). They indicated that this relationship might be of general use for flow over urban areas with the coefficient $C_u = 0.4 - 0.6$ being weakly dependent on morphology. Inagaki and Kanda (2008) related values of σ_u / u_* (at 2–4 block/building heights) to the ratio of the length scale of the inner layer to that of the outer layer. To compute this ratio, the aerodynamic roughness length, z_0, and the atmospheric boundary-layer depth, z_i, were adopted for the inner and outer layer length scales, respectively. The Comprehensive Outdoor Scale Model Experiment for Urban Climate (COSMO) showed that the values of σ_u / u_* decreased with increasing values of z_0 / z_i. In contrast, the values of σ_w / u_* varied little with z_0 / z_i, and the vertical velocity fluctuations were found to be insensitive to the outer scale eddies.

The height of measurement is important for the validity of turbulence scaling. Certainly, there is doubt on the suitability of MOST in the roughness sublayer (Barlow and Coceal 2009). For London, the roughness sublayer is of order 20–150 m in depth, so we expect our measurements at 190.3 m (see

later) to be above the roughness sublayer. Now, the rule-of-thumb value for the depth of the surface layer is $0.1z_i$, and as the roughness sublayer deepens (compared to the boundary-layer depth) some authors suggest that an inertial sublayer might not exist (Rotach 1999). Note also, Kaimal and Finnigan (1994) suggested a matching layer, in which z (rather than z_i) is the important length scale, even where buoyancy is important (i.e. for large L). Since there are so few urban mixed-layer studies (Roth 2000), the theory on the transition from the roughness sublayer to the mixed layer remains little supported by observations.

The purpose of the present paper is to examine the validity of several surface-layer and mixed-layer similarity relationships using sonic anemometer data taken at 190.3 m above ground level in central London. In the following sections, the measurement site and the available dataset are introduced. Similarity relationships are then tested (based on scales u_*, w_*, Λ and z_i) that describe the relationships between fluxes and variances of wind components and temperature.

2 Experimental Set-up and Data Processing

A sonic anemometer (alongside a LI-COR 6262 infrared gas analyser for gaseous flux calculations; results not shown here[1]) was mounted with its head at height 190.3 m on a telecommunications tower (BT Tower) in west-central London (51.5215 °N, 0.1389 °W; Fig. 1). The anemometer was clamped to the top of an open lattice scaffolding tower of 18 m height on top of the main structure. The data analysed here were collected from October 2006 to May 2008. BT Tower is the tallest building within several kilometres of its surrounds (and the fourth tallest in London), with good exposure to winds in all directions. The three-component winds ($i = u, v, w$) and temperature (T; we assume that sonic temperature is sufficiently close to air temperature to not alter the results) from the sonic anemometer (R3–50, Gill Instruments Ltd, 0.01 m s^{-1} resolution and accuracy) were archived at 20 Hz. No corrections were applied to the data (such as path averaging, spectral loss or cosine response).

The effect of the BT Tower on the flow has been investigated previously (Barlow et al. 2009; Wood et al. 2009), and it has been shown that turbulence intensity, as a function of wind direction, was small and relatively constant, suggesting negligible wake turbulence from the lattice tower. For a 2004 dataset, the upward streamline deflection (ψ) was observed for all wind directions (mean of $\psi = 8°$), suggesting some deflection around the lattice and, more likely, the main tower. Prior to the present

---

[1] See Atmos Chem Phys Disc special issue 95 "Atmospheric chemistry and physics in the atmosphere of a developed megacity (London): the results of the REPARTEE experiments"

measurements, the sonic anemometer was redeployed on a boom of 1.5 m on the south-west corner of the lattice tower. In the present dataset, the deflection was reduced to $\psi = 5.8 \pm 3.3°$ (mean ± standard deviation of the 30-min dataset) and was taken into account by applying a streamwise rotation, using the double-rotation method (Wilczak et al. 2001) so that the mean vertical and spanwise wind speeds were defined as zero ($\bar{v} = \bar{w} = 0$) for each averaging period (30 min). Periods with extreme vertical deflection (beyond 2.5 standard deviations, hence satisfying $-2 < \psi < 14°$) are rejected, on the hypothesis that updraughts induced by the tower influence the background flow in such extreme periods. Mean deflection was positive for all wind directions (when binned into 45° wind direction sectors, mean ψ varied from 3.9–7.2°).

Data were analysed in periods of 30 min, following earlier work (Langford et al. 2010), and is expected to be long enough to capture most of the scales of turbulence contributing to fluxes across most periods. Data were subject to quality control: data are removed if (*i*) the period of 30 min was not complete; (*ii*) the percentage of spikes exceeded 0.5%; (*iii*) the spectra of u, v, w or T exhibited high-frequency noise; (*iv*) there was an extreme vertical rotation angle of greater than 2.5 standard deviations from the mean. Spikes were defined as short duration (< 0.1 s) and large amplitude[2] (> 5 standard deviations) fluctuations in the time series, resulting from random electronic noise or sensor error caused by rain or other airborne matter (such as biological agents). Altogether, the original data-set of 10,368 h was reduced to 6,447 h on 432 days (giving 12,933 periods of length 30 min) after the aforementioned quality assurance tests (histograms showed that there was no bias in the climatology towards certain days or seasons in the rejection of data points).

Means, variances and covariances were derived from the anemometer data to provide wind speed and direction, sonic temperature, and turbulent fluxes of heat and momentum. To identify spectral peaks, power spectra were calculated for two-hour periods of anemometer data using MATLAB's *psd* function. Log-log plots were prepared of $fS(f)$ as a function of f (where f is the natural frequency and S is the spectral energy density). The peak frequencies, $f_{\max}$, in the spectra of streamwise (u) and spanwise (v) horizontal velocity components were calculated by fitting a second-order polynomial in the frequency range 0.0003–0.1 Hz (cf. Christen 2005). Assuming Taylor's frozen turbulence hypothesis holds (e.g. Kaimal et al. 1982), and taking the associated mean wind speed, a peak wavelength was calculated, $\lambda_{\max} = \bar{U} / f_{\max}$.

---

[2] Absolute spikes (of $|u|$, $|v| > 60$ m s^{-1}; $|w| > 30$ m s^{-1} and $-20 < T < 60°$C) were first removed to avoid excessive contamination of the standard deviation used to find spikes relative to the data.

3 Site Description

The urban area of Greater London has a diameter of around 40–50 km (Fig. 1). Some notable features: 25 km west-south-west of the BT Tower is Heathrow airport and several reservoirs; 13 km south-west is Richmond Park; 2 km south-west is Hyde Park; 1 km north-west is Regent's Park (Fig. 2d); and 10 km east-south-east is Canary Wharf where most of the tallest buildings in London are located (Fig. 2b). Greater London has only minor topographical features since it is in the Thames Valley (mostly < 40 m above sea level), with the Thames Estuary 30 km east of central London and hills 30 km south (North Downs) and 50 km north-west (Chiltern Hills) of central London (both peak at 267 m above sea level). The land use within a few km of BT Tower is mostly parks, offices, shops and residences (no industrial areas).

Morphological data were available from the Virtual London dataset: a three-dimensional digital model of > 3.5 million buildings within the Greater London area, licensed to the Centre for Advanced Spatial Analysis (CASA) at University College London (Evans 2009), and developed within a project entitled: The Development of a Local Urban Climate Model and its Application to the Intelligent Design of Cities (LUCID). Building height information within the Virtual London dataset was collected in the summer of 2005, and covers approximately 1650 km². Building morphology information within the dataset was compiled using the Ordnance Survey's MasterMap® dataset and Infoterra's 1 m lidar dataset (the lidar provided a horizontal accuracy of 1 m and an absolute vertical accuracy of ±0.15 m root-mean-square error). Plan and frontal area density data were calculated by CASA in 1 km² gridboxes for the present study (Evans 2009; Padhra 2009). Plan and frontal area density ratios were related to zero-plane displacement (z_d) and aerodynamic roughness length (z_0) using expressions from Raupach (1994) and Macdonald et al. (1998), typically derived using an array of cube obstacles (see Padhra 2009 for further details).

A flux source-area model (Schmid 1997; http://www.indiana.edu/~climate/SAM/) was used to estimate the surface upwind of the tower that defined the fetch for the measurements at 190.3 m during neutral conditions (further, spatial variability in roughness and heat flux was not considered). Fig. 1 shows circles of radii 1 and 10 km, pertaining to the 10 and 90% probability contours. Using the CASA 1 km² gridboxes, within 1–10 km of the tower the mean building height was calculated as 8.8 ±3.0 m (and the peak value of a gridbox was 26.5 m); beyond 10 km, most of suburban Greater London the mean building height was 5.6 ±1.8 m. Hence, the sensor was at a height ≈ 22 times the mean building height upwind of the tower (1–10 km). Padhra (2009) estimated that roughness lengths in London peaked at ≈ 2.9 m, but are more typically 0.87 ± 0.48 m over central London and 0.27 ± 0.21 m outside the 10 km radius from the tower. Large parks (such as Richmond Park) showed roughness lengths of ≈ 0.35 m. Zero-plane displacements within 10 km of the BT Tower were calculated as 4.3 ± 1.9 m. Given the great height of the sensor, at 190.3 m, in comparison to the

displacement height ($z \gg z_d$), the accuracy of the displacement height has minimal impact on the results when expressed in terms of $z' = z - z_d$.

4   Results and discussion

4.1 Climatology

Using the 12933-period dataset (each of length 30 min), south-west was the most frequently occurring wind direction (Fig. 3a) and the least frequent wind direction was from the south-east, consistent with the general pattern typical for the United Kingdom (Dore et al. 2006). Wind speed (Fig. 3c) ranged from zero to 20 m s^{-1} with a mode of 7 m s^{-1}. Stability was calculated as $\zeta = z'/\Lambda$, where the locally-scaled Obukhov length was calculated as $\Lambda = -u_*^3 / (\kappa g (\overline{w'T'})/T)$, $g = 9.8$ m s^{-2} is acceleration due to gravity, $u_*^2 = \sqrt{\overline{u'w'}^2 + \overline{v'w'}^2}$ (where $\overline{u'w'}$ and $\overline{v'w'}$ are covariances; u' and v' are fluctuations about the means), and z' = 190.3 m $-$ 4.3 m. During neutral conditions (defined as $|\zeta| < 0.1$) a similar wind direction distribution holds, but the wind speed distribution has a mode of about 10 m s^{-1}. Mean wind speeds were greatest for directions from the south-west and least from the east (Fig. 3b). Half of the sectors' day-to-night means agreed within confidence intervals, however many of the westerly sectors recorded greater wind speeds by night than day (an investigation of potential diurnal circulations over London could be worthwhile).

The number of unstable cases, defined in terms of *local* stability at 190.3 m, was about three times that for the stable cases (Fig. 4). The number of unstable cases at night was almost equal to the number during daytime, consistent with the heat output from the city. Some stable periods were observed during daytime, although only nine days were identified where the daytime was stable on average in terms of mean and median 30-min values (these were associated with seven synoptic weather events—only one of which was in summer—typically freezing fog layers in anticyclonic conditions). In comparison with the present dataset, measurements taken above flat rural terrain (Cabauw, the Netherlands, in 1996) at 180 m showed twice as many very stable ($|L| > 200$ m) cases compared to very unstable ones (Verkaik and Holtslag 2007).

The drag coefficient, $C_D = (u_*/\overline{U})^2$, in near-neutral stratification was greatest for flow from the east and south-east sectors than for the other sectors (Fig. 5), implying a rougher south-east upwind sector. Since C_D decreases with height above a given surface, BT Tower values (0.004–0.008) were smaller than other studies, as expected: e.g. (*i*) Nanjing rooftop at 22 m (Liu et al. 2009) with mean value of 0.04; (*ii*) New York City high rooftops (Hanna and Zhou 2007) with values of 0.01–0.03; and (*iii*)

Oklahoma City on an 83-m tower (Lundquist et al. 2004) with values of 0.004–0.03. The BT-observed values are those determined from the morphological data using $C_D = \kappa^2 \ln\left((z - z_d)/z_0\right)^{-2}$. The relevant upwind source areas were estimated using the flux source-area model developed by Schmid (1997). Fig. 5 shows that the correspondence is reasonable in terms of the average C_D values across all wind directions; however there are significant differences for certain wind direction sectors. A similar approach was employed by Al-Jiboori and Fei (2005) in Beijing and Liu et al. (2009) in Nanjing. The present study agrees with Liu et al. (2009), who concluded that the results from four morphological models recommended by Grimmond and Oke (1999) were very similar in predicting z_0 and z_d.

4.2 Wind Variances

Following the relationships used by Quan and Hu (2009), $\sigma_i / u_* = a_i (1 - b_i \zeta)^{c_i}$ and $\sigma_T / T_* = a_T (1 - b_T \zeta)^{-c_T}$, the coefficients a_i, a_T, b_i, b_T, c_i and c_T were determined for the present dataset and are shown in Table 3, assuming a value of $c_i = c_T = 0.33$ for unstable conditions ($i = u, v, w$). Normalized standard deviations of wind components were plotted as a function of z'/Λ together with formulations for a generic surface layer and other urban datasets (Fig. 6).

The σ_i / u_* values for neutral conditions ($|\zeta| < 0.1$) over London were found to be 2.3, 1.85 and 1.35 for u, v and w respectively (see also Martin 2009), values that are similar to those for simpler terrain shown in Table 1. One might note, though, that the values from the stable side were greater than those from the unstable side as ζ approaches zero; which is perhaps an artefact of the fitting process (others have similar results, e.g. Quan and Hu 2009). The dependence (for unstable stratification) of σ_u / u_* on stability was less pronounced than that of σ_v / u_*; the stability effect was most pronounced on σ_w / u_*.

Formulations for σ_i / u_* derived from the present London data for unstable conditions were similar to those for the surface layer over simpler terrain with a weaker dependence on stability. This agrees with the results of Christen (2005), who found that the best-fit line to all three normalized velocity standard deviations lies below the classical rural surface-layer formulation and the differences between measured urban values and the surface-layer prediction increases with distance above the roofs. In stable conditions, the London data showed a dependence on ζ. A similar trend is increasingly found across many terrain types, for example: 47-m urban measurements in Beijing

(Quan and Hu 2009), a 25-m tower in suburban Turin (Mortarini et al. 2009), and a 15-m tower in a valley in an area of rough and forested terrain in southern Brazil (Moraes et al. 2005).

Perhaps an appropriate scaling of σ_u / u_* should use z_i / Λ; Panofsky et al. (1977) found that $\sigma_u / u_* = (a + b z_i / L)^{1/3}$ is in agreement with observations taken over several rural sites with $a = 12$ and $b = 0.5$ (L is the Obukhov length). The method used to estimate z_i was to use the peaks in the energy spectra of u and v (Kaimal et al. 1982; Clarke et al. 1982; Liu and Ohtaki 1997), found as described in Section 2. The relations of Liu and Ohtaki (1997) were used: $z_i = 0.8 \overline{U} / f_{max}^u$ and $z_i = 0.75 \overline{U} / f_{max}^v$ (N.B. the coefficient of 0.8 for the u spectrum is different from that stated in Liu and Ohtaki (1997), where 0.53 was used and was possibly erroneous; see Vittal Murty et al. 1998). In the present dataset, z_i was estimated by taking the arithmetic mean of values calculated from both u and v spectra. Fig. 7 shows the Panofsky et al. (1977) expression fitted to the London dataset ($a = 5.6$ and $b = 1.2$), giving greater σ_u / u_* values than for the rural case as $z'/L \to -\infty$ and smaller values as $z'/L \to 0$.

Mixed-layer scaling was also applied, using the mixed-layer depth (z_i) and convective velocity scale (w_*), where $w_*^3 = \dfrac{g}{T} \, \overline{w'T'}_0 \, z_i$. The mixed-layer depth and corresponding w_* were calculated from spectral data of length two hours (instead of 30-min), and initially taking local values of both $\overline{w'T'}$ and T at 190.3 m. The measured σ_w^2 / w_*^2 values are plotted against z'/z_i for strongly unstable conditions ($\zeta < -0.5$) (Fig. 8) with some relationships from the literature: viz.

$$\left(\frac{\sigma_w}{w_*} \right)^2 = 1.2 \left(\frac{z'}{z_i} \right)^{2/3} \left(1 - 0.9 \frac{z'}{z_i} \right) + \left(\frac{u_*}{w_*} \right)^2 \left(1.8 - 1.4 \frac{z'}{z_i} \right), \tag{1}$$

$$\left(\frac{\sigma_w}{w_*} \right)^2 = 1.17 \left(\frac{z'}{z_i} (1 - \frac{z'}{z_i}) \right)^{2/3}, \tag{2}$$

$$\left(\frac{\sigma_w}{w_*} \right)^2 = 2.5 \left(\frac{z'}{z_i} \right)^{2/3} \left(1 - 0.91 \frac{z'}{z_i} \right), \tag{3}$$

$$\left(\frac{\sigma_w}{w_*} \right)^2 = 1.8 \left(\frac{z'}{z_i} \right)^{2/3} \left(1 - 0.8 \frac{z'}{z_i} \right)^2, \tag{4}$$

where Equations 1–4 are from Brost et al. (1982), Sorbjan (1989), Wilczak and Phillips (1986), and Lenschow et al. (1980), respectively. The Wilczak and Phillips (1986) formulation was derived from the Boulder Atmospheric Observatory's 300-m tower data (over mixed land-use terrain in Colorado).

Equation 1 includes an additional term for the mechanical generation of turbulence. Equation 4 is based on aeroplane measurements over the East China Sea and the formulation peaks at about $z'/z_i \approx 0.3$, whereas Equation 2 peaks at $z'/z_i = 0.5$, although the maximum value of σ_w^2/w_*^2 is similar in both formulations.

Given that the BT Tower instruments are at a considerable height above the surface, the surface heat flux would be greater than the local value at 190.3 m. The surface heat flux was estimated from the data obtained at 190.3 m by assuming a linear relationship between heat flux and height ($\overline{w'T'}_z = \overline{w'T'}_0 \left(1 - 1.2z/z_i\right)$, see Stull (1988), p. 370). The new σ_w^2/w_*^2 curve using this estimated surface heat flux (Fig. 8) shows a similar structure to the Lenschow et al. (1980) relation, with the maximum height of $(z'/z_i)_{max} \approx 0.35$, and the maximum value of $(\sigma_w^2/w_*^2)_{max} \approx 0.4$: which is quite similar to the value (of 0.44) found by Caughey and Palmer (1979) over rural terrain.

The vertical profiles of normalized standard deviation of the streamwise (Fig. 8a) and spanwise wind (not shown) components were similar to each other. The Wilczak and Philips (1986) formulation, based on the Boulder Atmospheric Observatory (BAO) tower measurements, is also depicted for comparison (Fig. 8a; assuming σ_u^2/w_*^2 and σ_v^2/w_*^2 have similar vertical profiles):

$$\frac{\sigma_v}{w_*} = 0.74\left(0.5\left\{2 - \left(\frac{z'}{z_i}\right)^{1/2}\right\} + 0.3\left(\frac{z'}{z_i}\right)^{1/2}\right)^{1/2}. \tag{5}$$

The London data showed only a weak dependence on z'/z_i. A similar profile was obtained for the Minnesota data (Caughey and Palmer 1979) but the London data have larger values. Using the estimate of surface heat flux, σ_u^2/w_*^2 becomes near constant with height as would be expected in a convective boundary layer. This suggests that the estimation of surface heat flux by the method above is a reasonable approximation in a convective boundary layer.

4.3 Temperature Variance

Similar to the surface-layer relationships for the standard deviation of the wind, several formulations have been suggested for temperature, σ_T/T_*. The values of σ_T/T_* show a dependence on stability for both unstable and stable conditions (Fig. 9a, b). The fitted values (with fixed exponent –0.33 for unstable conditions) in Table 3 are similar to the coefficient suggested by Quan and Hu (2009) shown in Table 1. The data were skewed and thus the bin-averaged mode (not shown) exhibited a smaller magnitude than the fitted curve during unstable conditions. The fitted curve diverges in the approach

to neutral conditions, demonstrating the difficulty in using T_* as a temperature scale when heat flux is near-zero.

Some (Tampieri et al. 2009, Kanda and Moriizumi 2009) have argued that temperature fluctuations do not become zero as the heat flux approaches zero because of unsteadiness and heterogeneity in the boundary layer "and in order to avoid anomalous results associated with small turbulence fluxes" (Kanda and Moriizumi 2009), the criterion used for sub-sampling the data for temperature variance analysis was $\overline{w'T'} > 0.05$ K m s^{-1}. Wilson (2008) employed $\overline{w'T'} > 0.05$ K m s^{-1} in the analysis of the universality of Monin-Obukhov similarity theory. For London data, the 0.01 K m s^{-1} threshold removed 29% of the database, whilst the 0.05 K m s^{-1} threshold removed 74%. Whilst the choice of threshold might be arbitrarily applied, the data rejection rate suggests that temperature variance scaling is only relevant for moderately to strongly convective conditions, and the scaling breaks down in near-neutral conditions.

Using mixed-layer similarity scaling, σ_T^2 / θ_*^2 values as a function of non-dimensionalized height are shown in Fig. 10 (where $\theta_* = \overline{(w'T')}_0 / w_*$); and for comparison, the Sorbjan (1989) fit from a rural surface and Lenschow et al. (1980) over the East China Sea are used, respectively,

$$\frac{\sigma_T^2}{\theta_*^2} = 2\left(1 - \frac{z'}{z_i}\right)^{4/3}\left(\frac{z'}{z_i}\right)^{-2/3} + 0.94\left(1 - \frac{z'}{z_i}\right)^{-2/3}\left(\frac{z'}{z_i}\right)^{4/3}, \tag{6}$$

$$\frac{\sigma_T^2}{\theta_*^2} = 1.8\left(\frac{z}{z_i}\right)^{-2/3}. \tag{7}$$

The London data have greater values compared with Sorbjan (1989)—obtained over rural terrain— but with a similar profile decreasing up to ≈ 0.5 z'/z_i. At the middle of the mixed layer (0.5 z'/z_i), the BT Tower data show $\sigma_T^2 / \theta_*^2 \approx 2 - 3$ using surface heat-flux estimates (and values around 10 based on the local heat flux), in comparison with $\sigma_T^2 / \theta_*^2 = 3$ observed over rural terrain from aircraft measurements (Caughey and Palmer 1979). Aircraft data (altitudes of 200–1000 m) over Philadelphia gave $\sigma_T^2 / \theta_*^2 = 8$ (Roth 2000).

4.4 Turbulent Transfer Efficiency

Turbulent correlation coefficients, a measure of the efficiency of turbulent transfer, are defined as (e.g. Roth 1993):

$$r_{uw}(\zeta) = \frac{\overline{u'w'}}{\sigma_u \sigma_w}, \tag{8}$$

11

$$r_{vw}(\zeta) = \frac{\overline{v'w'}}{\sigma_v \sigma_w}, \tag{9}$$

$$r_{wT}(\zeta) = \frac{\overline{w'T'}}{\sigma_w \sigma_T}, \tag{10}$$

where r_{uw}, r_{vw} and r_{wT} are the correlation coefficients for momentum and heat transfer. Their values can vary between 1 and –1. Knowledge of these coefficients are useful in estimating fluxes as inputs for dispersion models from mean winds and temperatures measured at one level (e.g. Qian et al. 2009).

During very unstable conditions the correlation coefficient for momentum was small (Fig. 11a, c) and the correlation coefficient for heat was large (Fig. 11e), whereas in neutral conditions the momentum correlation coefficients were greater: ≈ 0.3 and 0.1 for $\overline{u'w'}$ and $\overline{v'w'}$ respectively. The heat-flux correlation coefficient tended to 0.4 for very unstable cases ($\zeta < -1$), and 0.2–0.4 for $10 > \zeta > 1$. This coefficient increased strongly from neutral conditions ($|\zeta| < 0.1$) to unstable/stable conditions.

A review of typical values is presented in Table 4. Measurements taken under neutral to slightly unstable or stable conditions show $|r_{uw}| \approx 0.35$ over rural terrain, 0.1–0.4 over residential areas (*c*. 20-m high measurements), 0.3 over wetland (25-m high measurements), 0.3 over hilly terrain (aeroplane data) and 0.2–0.3 over urban areas (325-m tower). The $|r_{uw}|$ data show only small differences between the various sites. The heat-flux correlation coefficient was about 0.5 (unstable conditions) over rural terrain, similar to data taken over residential areas, but somewhat higher than those measured over wetland or hilly terrain. Data from high towers over urban areas show $|r_{wT}| \approx 0.2$ over Beijing, and higher values (0.4) over London in unstable conditions. During stable conditions, both datasets show $|r_{wT}| \approx 0.15 - 0.2$ (Fig. 11f).

These quantities above urban areas still appear to have some variation between different studies. The near-neutral London cases agree better with Filho et al. (2008), whilst away from neutral there is more agreement with Al-Jiboori (2008).

The ratio between the heat exchange and the momentum transfer correlation coefficients reach values greater than 10 (unstable stratification) and less than 1 close to neutral conditions. In stable conditions the ratio reach values of 10, consistent with Al-Jiboori (2008).

5   Conclusions

Monin-Obukhov similarity theory relationships generally apply for flat/rural sites, and are thus used in parameterizations of momentum, mass and energy in the atmospheric boundary layer (e.g. numerical models that simulate flow and diffusion). There is an ongoing effort to assess the applicability of scaling laws in urban flows, and in this study, the validity of several similarity relationships was tested for an urban site: namely sonic anemometer data obtained at 190.3 m atop the BT Tower in central London.

Surface-layer scaling, using locally-defined values of variances and covariances, was tested. Normalized wind standard deviations were found to follow Monin-Obukhov similarity theory well in both unstable and stable stratification, with values of σ_i / u_* ($i = u, v, w$) in neutral conditions found to be 2.3, 1.85 and 1.35 respectively, not dissimilar to those found over rural terrain. Increased values were found for $|\zeta| > 0.1$. The normalized temperature standard deviation showed more scatter but still collapsed as a function of the stability parameter, ζ, for all but near-neutral conditions. A large number of stable flows were seen in the climatology of these data at 190.3 m, perhaps indicating that there is decoupled flow between 190.3 m and the near-surface flow: that is, the near-surface flow is stable much less often (further study is planned by comparing rooftop, tower-top and lidar measurements).

Mixed-layer scaling was tested, using the mixed-layer depth z_i (estimated from spectra of the horizontal wind components) and the convective velocity scale w_* (defined (*i*) at 190.3 m, and (*ii*) adjusted to give a near-surface estimate of heat flux). Vertical and horizontal wind variances behaved similarly to observations in rural/flat terrain, particularly when the surface-adjusted w_* was used. The normalized temperature variance, σ_T^2 / θ_*^2 was similar to previous results.

The correlation coefficients for momentum were small under strong stratification but increased quite steeply toward neutral conditions. This behaviour was broadly in agreement with both an urban and rural dataset. The correlation coefficient for heat (r_{wT}) was large and constant for $|\zeta| > 0.1$ and decreased towards neutral conditions. The present results agree better with the rural dataset, in contrast with the previous urban dataset (Aljiboori) where constant r_{wT} was found.

Some key conclusions can be drawn:

1. Using local scaling, many of the generic similarity relationships were suitable for describing the present dataset, implying that locally-normalized turbulence at high levels above a large

urban area behaves not dissimilarly to that above simpler terrain. The Obukhov length has proven useful as a *local* length scale. Modelling approaches (such as numerical weather prediction), which assume Monin-Obukhov similarity theory to hold above an urban boundary layer, are thus reasonable. The caveat is that for London, Monin-Obukhov similarity theory is not complicated by too many factors, since London is quite flat and there are consistent building heights across a wide area (Evans 2009). This produces a longer upwind fetch than for some other cities with more variable building heights. Hence, the London boundary layer is likely to be in equilibrium with the surface.

2. The BT Tower is a well-exposed site, in the centre of London (with a city-scale fetch), and its height ensures that one can create a pseudo profile of the mixed layer (since a range in z'/z_i was observed) for the testing of mixed-layer similarity. The roughness sublayer might be relatively shallow compared with other cities; hence, the sensor height is likely to have been above the roughness sublayer most of the time. The broad agreement of the statistics with previous urban results (e.g. Roth 2000) suggests that our methodology for dealing with any disturbance by the platform itself is reasonable (although wind-tunnel tests are ongoing).

References

Al-Jiboori MH (2008) Correlation coefficients in urban turbulence. Boundary-Layer Meteorol 126:311–323

Al-Jiboori MH, Fei H (2005) Surface roughness around a 325-m meteorological tower and its effect on urban turbulence. Adv Atmos Sci 22:595–605

Al-Jiboori MH, Xu Y, Qian Y (2002) Local similarity relationships in the urban boundary layer. Boundary-Layer Meteorol 102:63–82

Barlow JF, Coceal O (2009) A review of urban roughness sublayer turbulence. UK Met Office Technical Report no. 527, 68 pp

Barlow JF, Dobre A, Smalley RJ, Arnold SJ, Tomlin AS, Belcher SE (2009) Referencing of street-level flows measured during the DAPPLE 2004 campaign. Atmos Environ 43:5536–5544

Brost RA, Wyngaard JC, Lenschow DH (1982) Marine stratocumulus layers. Part II: Turbulence budgets. J Atmos Sci 39:818–836

Caughey SJ, Palmer SG (1979) Some aspects of turbulence structure through the depth of the convective boundary layer. Q J Roy Meteorol Soc 105:811–827

Chang S, Huynh G, Tofsted D (2009) Turbulence characteristics in Oklahoma City measured from an 83-meters pseudo tower. Eighth Symposium on the Urban Environment, Phoenix, Arizona, January 12–15

Christen A (2005) Atmospheric turbulence and surface energy exchange in urban environments. PhD thesis, Faculty of Science, University of Basel, 142 pp

Clarke CF, Ching JKS, Godowich JM (1982) A study of turbulence in an urban environment. EPA technical report, EPA 600-S3-82-062

Dore A, Vieno M, Fournier N, Weston KJ, Sutton MA (2006) Development of a new wind-rose for the British Isles using radiosonde data, and application to an atmospheric transport model. Q J Roy Meteorol Soc 132:2769–2784

Evans S (2009) 3D cities and numerical weather prediction models: An overview of the methods used in the LUCID project. CASA Working Paper 148, 19 pp

Filho EPM, Sa LDA, Karam HA, Alvala RCS, Souza A, Periera MMR (2008) Atmospheric surface layer characteristics of turbulence above the Pantanal wetland regarding the similarity theory. Agric For Meteorol 148:883–892

Grimmond CSB, Oke TR (1999) Aerodynamic properties of urban areas derived from analysis of surface form. J Appl Meteorol 38:1262–1292

Hanna S, Zhou Y (2007) Results of analysis of sonic anemometer observations at street level and rooftop in Manhatan. 6th international conference on urban air quality, Limassol, Cyprus, March 27–29, 4 pp

Inagaki A, Kanda M (2008) Turbulent flow similarity over an array of cubes in near-neutrally stratified atmospheric flow. J Fluid Mech 615:101–120

Kaimal JC, Eversole RA, Lenschow DH, Stankov BB, Kahn PH, Businger JA (1982) Spectral characteristics of the convective boundary layer over uneven terrain. J Atmos Sci 39:1098–1114

Kaimal JC, Finnigan JJ (1994) Atmospheric boundary layer flows: their structure and measurements. Oxford University Press, New York, USA, 289 pp

Kanda M, Moriizumi T (2009) Momentum and heat transfer over urban-like surfaces. Boundary-Layer Meteorol 131:385–401

Langford B, Nemitz E, House E, Phillips GJ, Famulari D, Davison B, Hopkins JR, Lewis AC, Hewitt CN (2010) Fluxes and concentrations of volatile organic compounds above central London, UK. Atmos Chem Phys 10:627–645

Lenschow DH, Wyngaard JC, Pennell WT (1980) Mean-field and second moment budgets in a baroclinic, convective boundary layer. J Atmos Sci 37:1313–1326

Liu G, Sun J, Jiang W (2009) Observational verification of urban surface roughness parameters derived from morphological models. Meteorol Appl 16:205–213

Liu X, Ohtaki E (1997) An independent method to determine the height of the mixed layer. Boundary-Layer Meteorol 85:497–504

Lundquist JK, Leach M, Gouveia F (2004) Turbulent kinetic energy in the Oklahoma City urban environment. 5th conference on urban environment, Vancouver, BC, August 23–27, 5 pp

Macdonald RW, Griffiths RF, Hall DJ (1998) An improved method for estimation of surface roughness of obstacle arrays. Atmos Environ 32:1857–1864

Martin C (2009) Transportation of Urban Ultrafine Particles in Four European Cities. PhD thesis, University of Manchester, 282 pp

Moraes OLL, Acevedo OC, Degrazia GA, Anfossi D, da Silva R, Anabor V (2005) Surface layer turbulence parameters over complex terrain. Atmos Environ 39:3103–3112

Moriwaki R Kanda M (2006) Local and global similarity in turbulent transfer of heat, water vapour and CO_2 in the dynamic convective sub-layer over a suburban area. Boundary-Layer Meteorol 120:163–179

Mortarini L, Ferrero E, Richiardone R, Falabino S, Anfossi D, Trini Castelli S, Carretto E (2009) Assessment of dispersion parameterizations through wind data measured by three sonic anemometers in a urban canopy. Adv Sci Res 3:91–98

Padhra A (2009) Estimating the sensitivity of urban surface drag to building morphology. PhD thesis, University of Reading, UK, 143 pp

Panofsky HA, Tennekes H, Lenschow DH, Wyngaard JC (1977) The characteristics of turbulent velocity components in the surface layer under convective conditions. Boundary-Layer Meteorol 11:355–361

Qian W, Princevac M, Venkatram A (2009) Relationships between urban and suburban micrometeorological variables. Eighth Symposium on the Urban Environment, Phoenix, Arizona, January 12–15, 11 pp

Quan L, Hu F (2009) Relationship between turbulent flux and variance in the urban canopy. Meteorol Atmos Phys 104:29–36

Raupach MR (1994) Simplified expressions for vegetation roughness length and zero-plane displacement as functions of canopy height and area index. Boundary-Layer Meteorol 71:211–216

Rotach MW (1999) On the influence of the urban roughness sublayer on turbulence and dispersion. Atmos Environ 33:4001–4008

Roth M (2000) Review of atmospheric turbulence over cities. Q J Roy Meteorol Soc 126:941–990

Roth M (1993) Turbulent transfer relationships over an urban surface. II: Integral statistics. Q J Roy Meteorol Soc 119:1105–1120

Sato A, Michioka T, Takimoto H (2008) Field experiments of flow and dispersion within street canyons using outdoor urban scale model. 12th conference on harmonization within the atmospheric dispersion modelling for regulatory purposes, Cavtat, Croatia, October 6–9, 18 pp

Schmid HP (1997) Experimental design for flux measurements: Matching scales of observation and fluxes. Agric For Meteorol 87:179–200

Sorbjan Z (1989) Structure of the atmospheric boundary layer. Prentice Hall, New Jersey, USA, 317 pp

Stull RB (1988) An introduction to boundary layer meteorology. Kluwer Academic Publishers, Dordrecht, The Netherlands, 680 pp

Tampieri F, Maurizi A, Viola A (2009) An investigation on temperature variance scaling in the atmosphere surface layer. Boundary-Layer Meteorol 132: 31–42

Verkaik JW, Holtslag AAM (2007) Wind profiles, momentum fluxes and roughness lengths at Cabauw revisited. Boundary-Layer Meteorol 122:701–719

Vittal Murty KPR, Prasad GSSD, Sá LDA, Filho EPM, de Souza A, Malhi Y (1998) A Method to Determine the Height of the Mixed Layer from Spectral Peak Frequency of Horizontal Velocity. In: X Congresso Brasileiro de Meteorologia, 1998, Brasília. Anais do X Congresso Brasileiro de Meteorologia, 4 pp

Wilczak JM, Phillips MS (1986) An indirect estimation of convective boundary layer structure for use in pollutant dispersion models. J Climate Appl Meteor 25:1609–1624

Wilczak JM, Oncley SP, Stage SA (2001) Sonic anemometer tilt correction algorithms. Boundary-Layer Meteorol 99:127–150

Wilson JD (2008) Monin-Obukhov functions for standard deviations of velocity. Boundary-Layer Meteorol 129:353–369

Wood CR, Arnold SJ, Balogun AA, Barlow JF, Belcher SE, Britter RE, Cheng H, Dobre A, Lingard JJN, Martin D, Neophytou M, Petersson FK, Robins AG, Shallcross DE, Smalley RJ, Tate JE, Tomlin AS, White IR (2009) Dispersion experiments in central London: the 2007 DAPPLE project. Bull Am Meteorol Soc 90:955–969

Tables

Table 1 Non-dimensionalized standard deviations of the wind and temperature as a function of stability

Reference	σ_u / u_*	σ_v / u_*	σ_w / u_*	σ_T / T_*	Comments
Wesely et al. (1970)	n/a	n/a	n/a	$2(1-16\zeta)^{1/2}$	Unstable
Panofsky et al. (1977)	$(12+0.5\zeta)^{1/3}$	$(12+0.5\zeta)^{1/3}$	$1.3(1+3\zeta)^{1/3}$	n/a	Unstable
Roth (2000)	$1.98(1-0.33\zeta)^{0.56}$	$1.64(1-2.84\zeta)^{0.30}$	$1.12(1-2.48\zeta)^{0.33}$	$-3.03(1-24.4\zeta)^{-0.33}$	Unstable; urban review
Pahlow et al. (2001)	$2.3+4.3\zeta^{0.5}$	$2.0+4.0\zeta^{0.6}$	$1.1+0.9\zeta^{0.6}$	$0.05\zeta^{-1}+3$	Stable
Quan and Hu (2009)	$1.96(1+2.07\zeta)^{1/3}$	$1.80(1+1.78\zeta)^{1/3}$	$1.42(1+0.54\zeta)^{1/3}$	$3.0(\zeta)^{-1/3}$	Stable; urban terrain
	$2.03(1-0.50\zeta)^{1/3}$	$1.70(1-1.05\zeta)^{1/3}$	$1.33(1-1.27\zeta)^{1/3}$	$-1.5(-\zeta)^{-1/3}$	Unstable; urban terrain

Table 2 Some recent relationships between σ_i and u_* over urban areas for neutral and near-neutral conditions

Study	σ_u / u_*	σ_v / u_*	σ_w / u_*	Comments
Lundquist et al. (2004)	3	2.7	1.7	South sector of tower (7.8–83.2 m) in Oklahoma City; stratification not specified
Hanna and Zhou (2007)	[†] $\sigma_h = 5.27$		1.7	150–280 m rooftops in New York City; ($-2.5 < \zeta < -1$)
Kono et al. (2008)	2.5	2.3	1.47	Average values from 54 m tower; ($-4.2 < \zeta < 0.25$)
Sato et al. (2008)	2.74	2.41	1.29	Average values from COSMO (at 2 h); neutral
Chang et al. (2009)	2.4–1.8	2.2–1.4	1.5–1.2	7.8–83.2 m in Oklahoma City; neutral

[†] $\sigma_h = \sqrt{\sigma_u^2 + \sigma_v^2}$

Table 3 Fitted relationships for the non-dimensionalized standard deviations of the wind and temperature for London, see Figs 6 and 9

Condition	σ_u / u_*	σ_v / u_*	σ_w / u_*	σ_T / T_*
Unstable	$2.23(1-0.22\zeta)^{1/3}$	$1.78(1-0.57\zeta)^{1/3}$	$1.31(1-0.65\zeta)^{1/3}$	$-1.4\zeta^{-1/3}$

| Stable | $2.36(1+1.15\zeta)^{0.20}$ | $1.92(1+1.33\zeta)^{0.22}$ | $1.40(1+0.46\zeta)^{0.19}$ | $3.41\zeta^{-0.18}$ |

Table 4 Turbulent transfer coefficients over different surfaces (see equations 8–10)

| Study	Stable		Unstable		Comments
	$\lvert r_{uw}\rvert$	$\lvert r_{wT}\rvert$	$\lvert r_{uw}\rvert$	$\lvert r_{wT}\rvert$	
The present study	0.2–0.3	0.2–0.3	0.2–0.3	0.4	London
Al-Jiboori (2008)	0.2	0.14	0.2	0.24	47–280 m above urban area
Filho et al. (2008)	0.31	0.3	0.13–0.3	0.5	25 m above wetland
Kaimal and Finnigan (1994)	–	–	0.35	0.5	Rural terrain
Mengesha (1999)	0.1–0.2	0–0.2	0.2–0.4	0.1–0.6	Flight over hilly rural terrain
Moriwaki and Kanda (2006)	–	–	0.1–0.2	0.35–0.6	20 m above residential area
Roth (1993)	–	–	0.1–0.4	0.5–0.6	19 m over sub-urban area

Figure captions

Fig. 1 Greater London: rings are of radius 1 and 10 km from the BT Tower. Colours are mean building heights in 250 m grid squares; from the Virtual London dataset (Evans 2009), courtesy of CASA
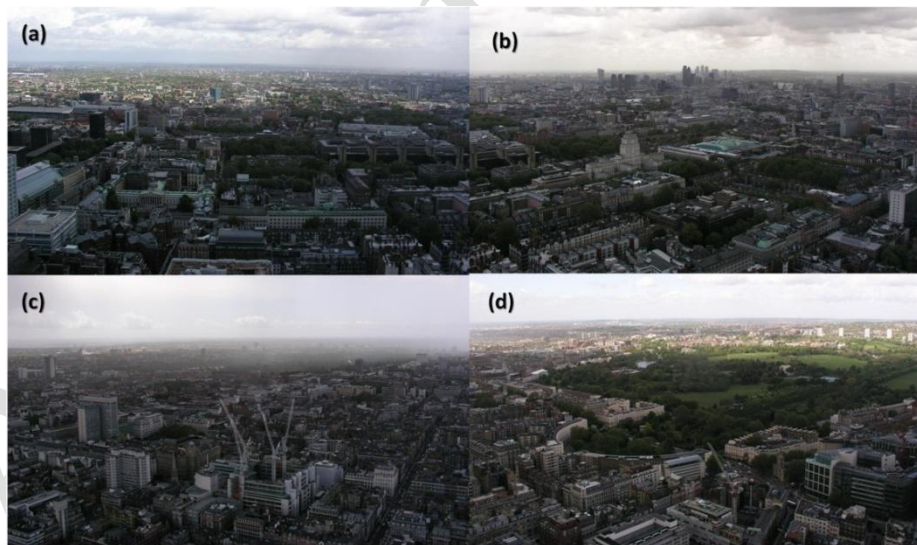
Fig. 2 View from the BT Tower at a height of 160 m looking north-eastwards (**a**), eastwards (**b**) towards the Central Business District (Canary Wharf, City of London), south-westwards (**c**) towards Hyde Park, and north-westwards (**d**) across The Regent's Park. Photographs taken in May 2009

Fig. 3 Frequency distributions of wind direction (**a**; neutral defined as $|\zeta| < 0.1$) and speed (**c**), and mean wind speeds in each 45° sector (**b**; confidence intervals, 95%, on the means are shown). All data included (i.e. 6446.5 hours between October 2006 and May 2008)

Fig. 4 Frequency histogram of stability (ζ) in 0.1 bins for nighttime (**a**) and daytime (**b**); and frequency of stability classes categorized by period of day (**c**), transition period was defined as two hours centred on sunrise or sunset, based on solar geometry. There were more nighttime than daytime data due to there being more winter than summer months in the dataset). All data included (i.e. 6446.5 hours between October 2006 and May 2008)

Fig. 5 Dimensionless drag coefficient, C_D, as a function of upwind sector for aerodynamic method, compared to morphologically-derived C_D (within the range 1–10 km upwind of the BT Tower) from Raupach (1994) and Macdonald et al. (1998). Confidence intervals (95%) of the means are shown. Aerodynamic data sub-sampled for neutral ($|\zeta| > 0.1$) and $\overline{U} > 1$ m s^{-1}

Fig. 6 Normalized standard deviations of u (**a–b**), v (**c–d**) and w (**e–f**) as a function of stability ($\zeta = z'/\Lambda$). The London curve is fitted for $0.03 < |\zeta| < 10$. The 30-min London values are shown as grey crosses (data sub-sampled for $\overline{U} > 1$ m s^{-1} and $\left|\overline{w'T'}\right| > 0.01$ K m s^{-1})

Fig. 7 For unstable conditions, σ_u / u_* as a function of z_i/Λ. The London fit is $\left(.62 - 1.25(z_i/\Lambda)\right)^{-1/3}$ and 30-min London values are shown as grey crosses (data sub-sampled for $\overline{U} > 1$ m s^{-1} and $\left|\overline{w'T'}\right| > 0.01$ K m s^{-1})

Fig. 8 Normalized standard deviations of u (**a**) and w (**b**) (kinematic heat flux at the BT Tower ($\overline{w'T'}_{190}$) and estimated for the surface ($\overline{w'T'}_0$) have been used to scale data) as a function of binned z'/z_i. Confidence intervals (95%) of the means are shown (data sub-sampled for daytime, cases of stronger convection ($\zeta < -0.5$), $\overline{U} > 1$ m s^{-1} and $\left|\overline{w'T'}\right| > 0.01$ K m s^{-1})

Fig. 9 Normalized standard deviation of temperature against stability ($\zeta = z'/\Lambda$): unstable (**a**) and stable (**b**). The London curve is fitted for $0.01 < |\zeta| < 10$. The 30-min London values are shown as grey crosses (data sub-sampled for $\overline{U} > 1$ m s^{-1} and $\left|\overline{w'T'}\right| > 0.05$ K m s^{-1})

Fig. 10 Normalized standard deviation of temperature (using kinematic heat flux at the BT Tower ($\overline{w'T'}_{190}$) and estimated for the surface ($\overline{w'T'}_0$) have been used to scale data) as a function of binned z'/z_i. Confidence intervals (95%) of the means are shown (data sub-sampled for daytime, $\overline{U} > 1$ m s^{-1} and $\left|\overline{w'T'}\right| > 0.05$ K m s^{-1})

Fig. 11 Momentum (**a–d**) and heat flux (**e–f**) correlation coefficients, and the ratio between heat flux and momentum transfer (**g–h**) as a function of stability ($\zeta = z'/\Lambda$). Confidence intervals (95%) of the means are shown (data sub-sampled for $\overline{U} > 1$ m s^{-1} and $\left|\overline{w'T'}\right| > 0.01$ K m s^{-1})

Figures and captions
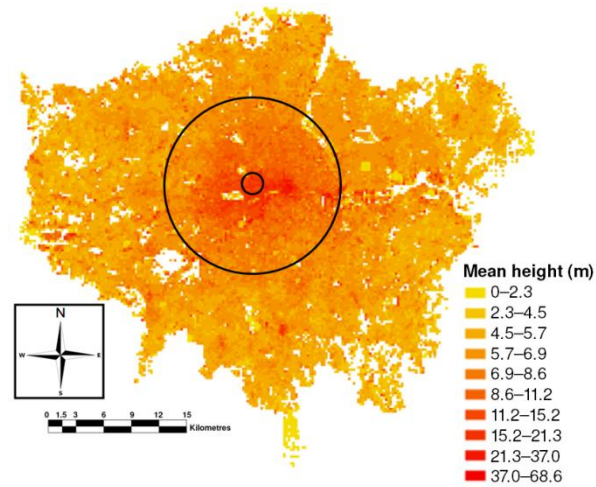
Fig. 7 Greater London. Rings are of radius 1 and 10 km from BT Tower. Colours are mean building heights in 250 m grid squares; from the Virtual London dataset (Evans 2009), courtesy of CASA.

Fig. 8 View from BT Tower at 160 m looking north-eastwards (**a**), eastwards (**b**) towards the Central Business District (Canary Wharf, City of London), south-westwards (**c**) towards Hyde Park, and north-westwards (**d**) across Regent's Park. Photographs taken in May 2009
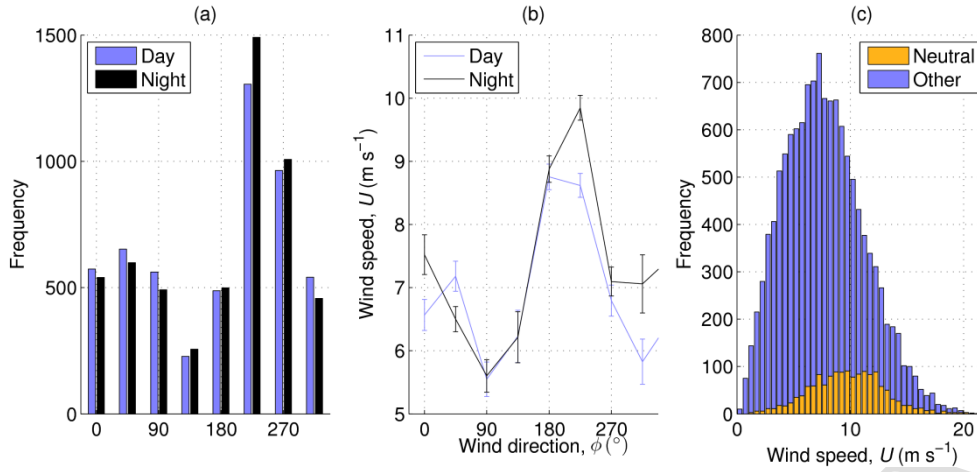
Fig. 9 Frequency distributions of wind direction (**a**; neutral defined as $|\zeta| < 0.1$) and speed (**c**), and mean wind speeds in each 45° sector (**b**; confidence intervals, 95%, on the means are shown). All data included (i.e. 6446.5 h between October 2006 and May 2008)
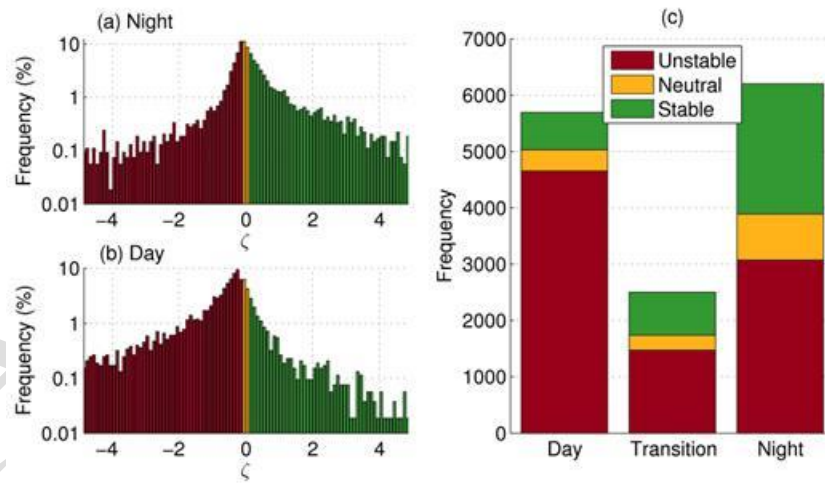
Fig. 10 Frequency histogram of stability (ζ) in 0.1 bins for night-time (**a**) and daytime (**b**); and frequency of stability classes categorized by period of day (**c**; transition period was defined as two hours centred on sunrise or sunset, based on solar geometry. There were more night-time than daytime data due to there being more winter than summer months in the dataset). All data included (i.e. 6446.5 h between October 2006 and May 2008)
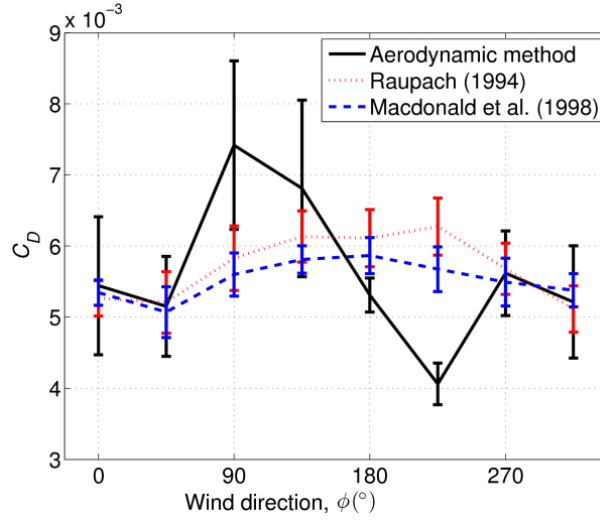
Fig. 11 Dimensionless drag coefficient, C_D, as a function of upwind sector for aerodynamic method, compared to morphologically-derived C_D (within the range 1–10 km upwind of BT Tower) from Raupach (1994) and Macdonald et al. (1998). Confidence intervals (95%) of the means are shown. Aerodynamic data sub-sampled for neutral ($|\zeta| > 0.1$) and $\overline{U} > 1$ m s^{-1}
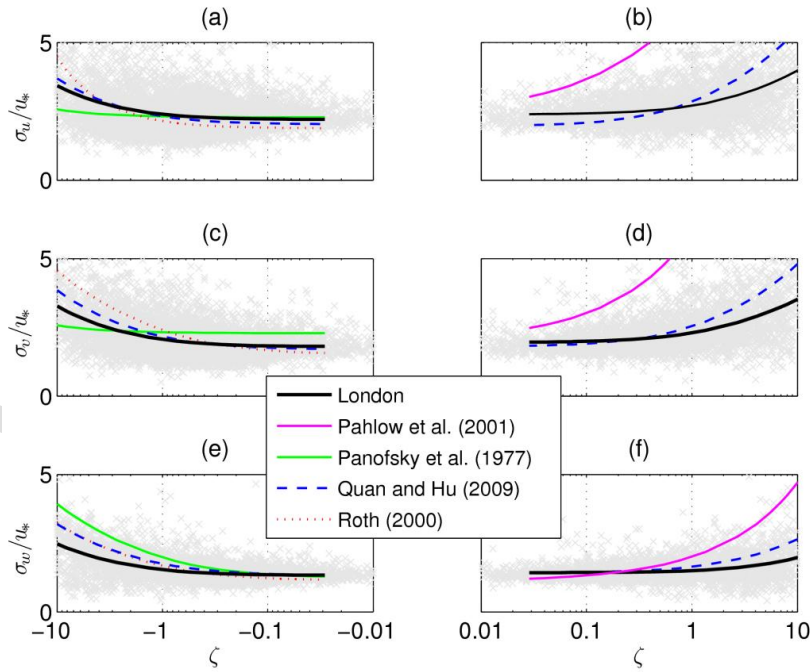

Fig. 12 Normalized standard deviations of u (**a–b**), v (**c–d**) and w (**e–f**) as a function of stability ($\zeta = z'/\Lambda$). The London curve is fitted for $0.03 < |\zeta| < 10$. The 30-min London values are shown as grey crosses (data sub-sampled for $\overline{U} > 1$ m s^{-1} and $|\overline{w'T'}| > 0.01$ K m s^{-1})

22

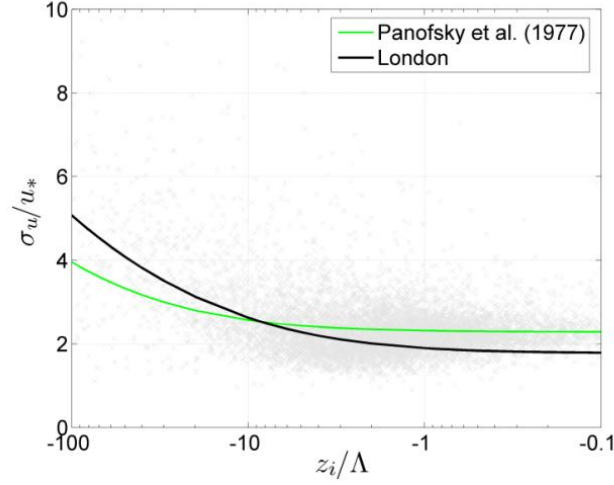**Fig. 7** For unstable conditions, σ_u / u_* as a function of z_i / Λ. The London fit is $4.62 - 1.25(z_i / \Lambda)^{1/3}$ and 30-min London values are shown as grey crosses (data sub-sampled for $\overline{U} > 1$ m s^{-1} and $\left|\overline{w'T'}\right| > 0.01$ K m s^{-1})
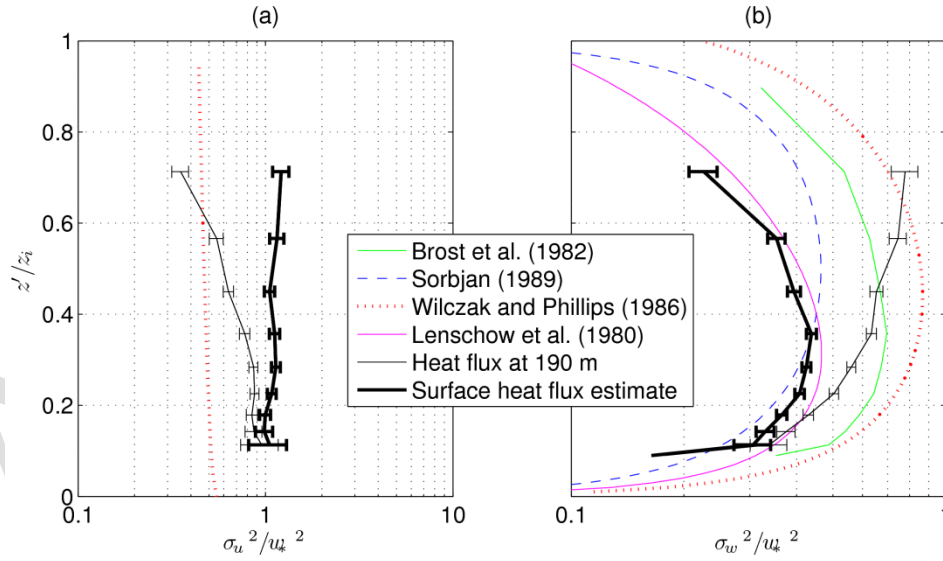

Fig. 8 Normalized standard deviations of u (**a**) and w (**b**) (kinematic heat flux at BT Tower ($\overline{w'T'}_{190}$) and estimated for the surface ($\overline{w'T'}_0$) have been used to scale data) as a function of binned z' / z_i. Confidence intervals (95%) of the means are shown (data sub-sampled for daytime, cases of stronger convection ($\zeta < -0.5$), $\overline{U} > 1$ m s^{-1} and $\left|\overline{w'T'}\right| > 0.01$ K m s^{-1})
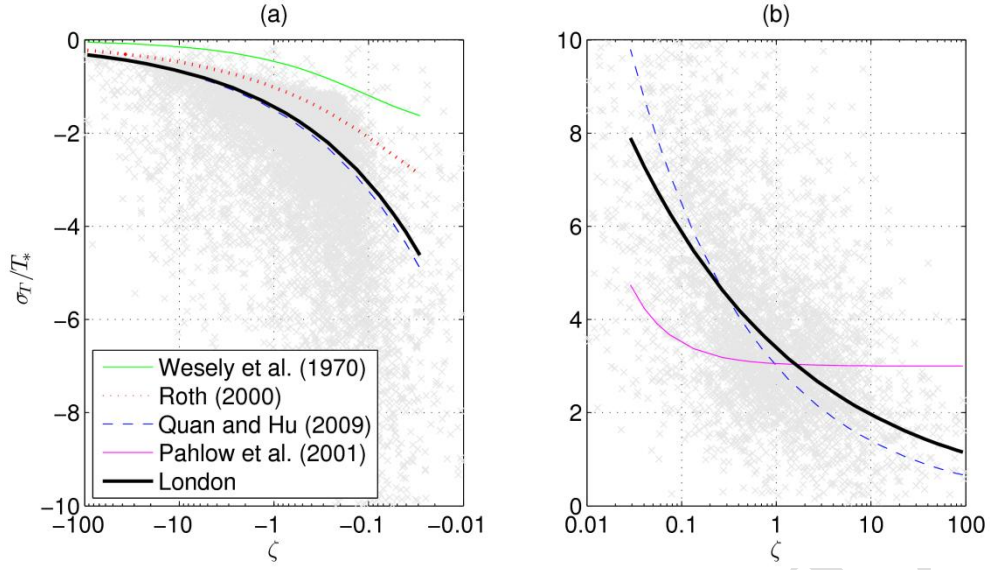
Fig. 9 Normalized standard deviation of temperature against stability ($\zeta = z'/\Lambda$): unstable (**a**) and stable (**b**). The London curve is fitted for $0.01 < |\zeta| < 10$. The 30-min London values are shown as grey crosses (data sub-sampled for $\overline{U} > 1$ m s^{-1} and $\left|\overline{w'T'}\right| > 0.05$ K m s^{-1})
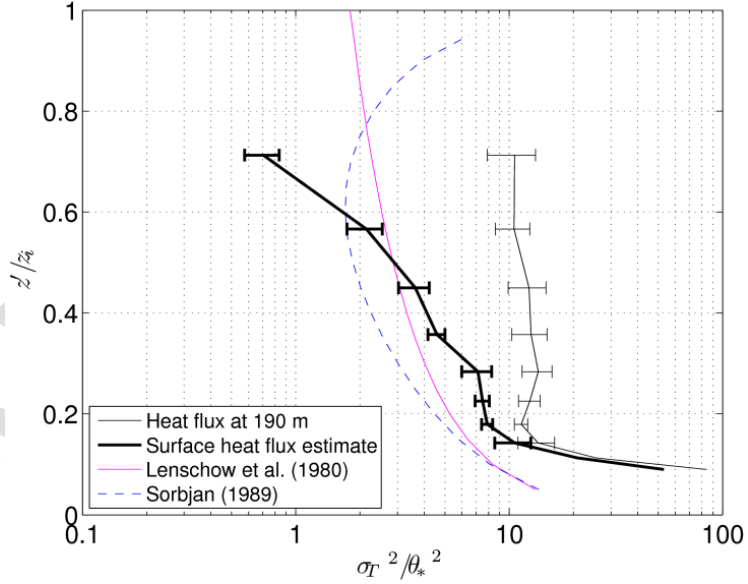

Fig. 10 Normalized standard deviation of temperature (using kinematic heat flux at BT Tower ($\overline{w'T'}_{190}$) and estimated for the surface ($\overline{w'T'}_0$) have been used to scale data) as a function of binned z'/z_i. Confidence intervals (95%) of the means are shown (data sub-sampled for daytime, $\overline{U} > 1$ m s^{-1} and $\left|\overline{w'T'}\right| > 0.05$ K m s^{-1})
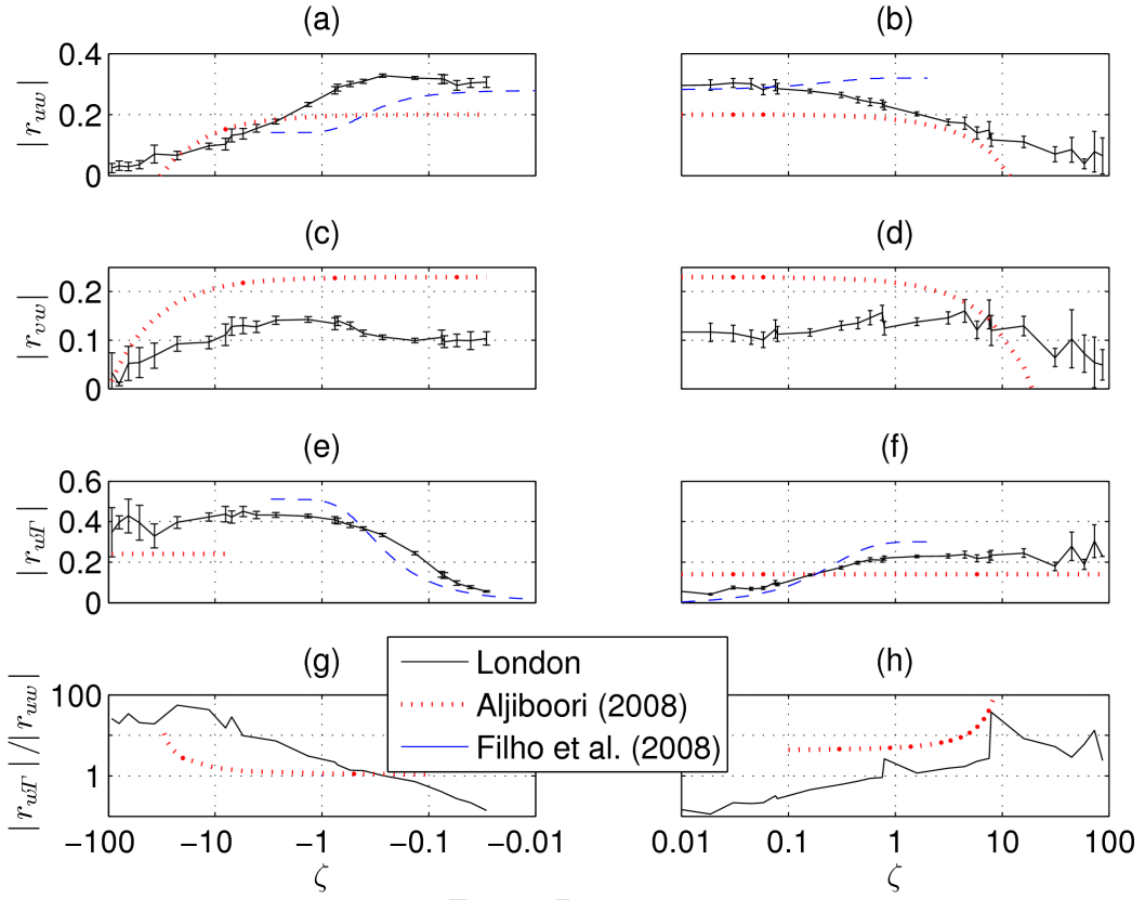
Fig. 11 Momentum (**a–d**) and heat flux (**e–f**) correlation coefficients, and the ratio between heat flux and momentum transfer (**g–h**) as a function of stability ($\zeta = z'/\Lambda$). Confidence intervals (95%) of the means are shown (data sub-sampled for $\overline{U} > 1$ m s^{-1} and $\left|\overline{w'T'}\right| > 0.01$ K m s^{-1})